JSEE Vol. 21, No. 3, 2019 DOI:10.48303/jsee.2019.241708

Design of Mass Isolated Structures with Consideration of Stability Constraints

Mohammad Boujary[1] and Mansour Ziyaeifar[2]*

1. Ph.D. Candidate, International Institute of Earthquake Engineering and Seismology (IIEES), Tehran, Iran
2. Assistant Professor of Structural Engineering Research Center, International Institute of Earthquake Engineering and Seismology (IIEES), Tehran, Iran,
*Corresponding Author; email: Mansour@iiees.ac.ir

Received: 18/05/2020
Accepted: 18/10/2020

ABSTRACT

Vertical mass isolation is one of the new techniques in the seismic design of structures that consists of two stiff and soft substructures connected by viscous dampers. Adding to the flexibility and energy dissipation potential of the system is the main feature of some new approaches in the seismic design of structures. Extra flexibility helps to reduce earthquake-induced forces and accelerations in the building and provides higher energy dissipation potential for the system (by creating large relative deformations in the structure). Mass subsystem possesses low lateral stiffness but carries the major part of the mass system. Stiffness subsystem, however, controls the deformation of the mass subsystem and attributes with much higher stiffness. In this paper, the aim is to find the limitation of the stability of a soft structure and to obtain the maximum period available for a soft structure. According to the studies, the most important obstruction in increasing the period of the soft structure, assuming control of its deformation by connecting to the stiff substructure, is to maintain the stability of the structure. In this paper, first, a relationship has been presented to calculate the period of the structure in terms of the stability factor that estimates the period of structure with good agreement by analytical results. This paper deals with presenting a procedure for designing the Mass Isolation System (MIS) with consideration of stability constraints. To this end, the paper presents mathematical solutions to calculate the period of the structure followed by proposing a design procedure of the soft substructure.

Keywords:
Mass isolation; Structural stability; P-Δ effect; Collapse prevention

1. Introduction

In conventional methods for seismic design of structures adopted by building codes [1-2], the structural deformation is controlled by increasing the stiffness of the structure while ductility and performance is controlled by its strength. Therefore, in severe earthquakes, plastic hinges are formed in structural elements, and large structural deformations occur. However, modern seismic control performance is often based on the flexibility and earthquake energy dissipation to the structure. In this way, the connection of two adjacent structures, which have a period difference, is investigated by the viscous damper in various papers, and the results show a significant decrease in the seismic behavior of both structures [3-6]. All of this research shows that if the frequencies of the two structures are close to each other, the efficiency of the dampers and the control strategy to improve the performance of the structures will be greatly reduced. This method can also be applied to a building by separating the lateral load system from the gravity load system, which can then be followed by a periodic difference (for example, to achieve a frequency ratio of 10 for the first mode period of

two structures). The proposed system is known as the Mass Isolation System (MIS) [5]. Such structures can be modeled as a simplified model according to Figure (1).

It is possible to divide the segregated model into two soft and stiff parts (see Figure 2) so that the major part of the mass in the left-hand structure (the mass subsystem or soft structure) and the major part of the stiffness in the right-hand structure (the stiffness subsystem or stiff structure) are concentrated. Two single degrees of freedom (SDOF) subsystems are connected to each other by a viscous damper *C*. The damper reduces the range of displacements of a mass subsystem, and the stiffness subsystem plays the role of the support of the energy dissipation mechanism [5-6]. Of course, in this category, special attention should be paid to the performance requirements of both soft and stiff structures and existing restrictions. Theoretically, the best design for both stiff and soft structures is that the period of the soft structure is taken as high as possible, so that it can be assumed this structure

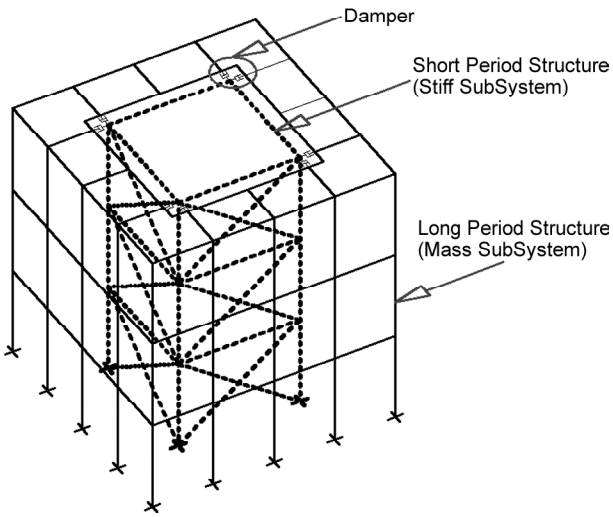

Figure 1. Simplified model of the mass isolation system.

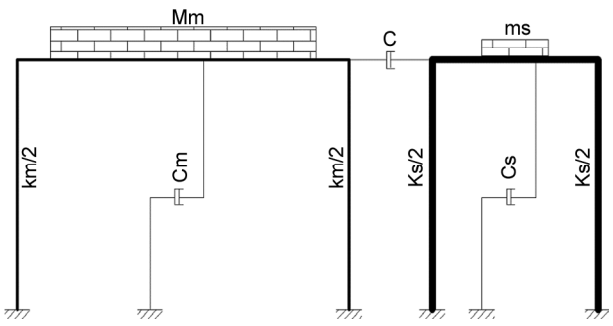

Figure 2. Two-mass modeling.

is designed exclusively for gravity forces and without the effects of lateral forces. On the other hand, the stiff structure, which plays the role of the support of the dampers system, must be somewhat rigid and hard to allow its displacement to be eliminated as far as possible. As a result, the stiff structure can be a supporter of the dampers, so that the design of this structure also requires special sensitivities.

The main purpose of this design approach is seismic energy dissipation by the damping interface between two subsystems, due to the relative displacement of the two stiff and mass subsystems. To achieve the Immediate Occupancy (IO) performance level, it is assumed that the structural drift ranges from 0.5% to 1.0% [7-8]. The maintenance of this performance limit is conditioned by the existence of intermediate dashpots that is able to maintain the displacement in the preserved range.

The concept of mass isolation is, in fact, a structural architectural idea that can be considered as the basis of design and is one of the methods to provide the experience of the high damped at a range of 20%. Mass isolation is more effective than other methods for increasing damping, in fact, providing this damping using other solutions, due to the limited speed and relative damper displacement, requires a high damping coefficient, which can cause such systems to be locked up.

In the isolated structures, the stiff structure is designed similar to the classical force-based design methods. Since this structure acts as a support for the reaction of the damper, during the earthquake it must be possible to withstand the forces of the soft structure (transmitted through the reaction of the damper). The design criterion for the soft structure should be based on the displacement control method, since the major part of the seismic forces in this part of the structure is transmitted to the stiff structure through dampers. In order to achieve the ideal state of the soft structure, its seismic load should be reduced, which leads to an increase in the period of the structure. It can be shown that there is always an inverse relationship between the period T and the stability factor, expressed as $T = \alpha\lambda^{-\beta}$, where the coefficients α and β are determined with respect to the height of the structure and other structural parameters, and λ from eigenanalysis of the structural stiffness matrix is determined by

taking into account the effects of P-Δ. Therefore, the aim of this paper is to provide a preliminary method for designing high damped structures (and especially mass isolation systems). In this process, considering the possibility of endangering the overall stability of the structure, first, considering the executive limitations and applying the safety factor, the minimum stability factor for moment frame structures is determined. Finally, a relationship is presented to calculate the period of moment frame structures, and then based on pushover analysis, numerical studies and selection of logical assumptions, an attempt has been made to provide an initial and simple method for designing high damped structures with limited deformation. The method of doing work is based on a combination of the nonlinear pushover and dynamic methods, taking into account the gravity load effects.

Table 1. Structural performance levels.

Elements	Immediate Occupancy (%)	Life Safety (%)	Collapse Prevention (%)
Concrete Moment Frames	0.8	1.6	3.2
Steel Moment Frames	0.56	2.0	4.0
Concrete Shear Walls	0.4	0.8	1.6
Braced Steel Frames	0.4	1.2	1.6
Unreinforced Masonry Infill Walls	0.08	0.4	0.48
Unreinforced Masonry Walls	0.24	0.48	0.8
Reinforced Masonry Walls	0.24	0.48	1.2

Table 2. Proportional importance factors [9].

Building Group	Important Factor
I	1.4
II	1.2
III	1.0
IV	0.8

2. Determining the Maximum Displacement of the Structure

In the design of the mass isolated structure, the deformation of the soft structure is very influential and critical and can cause the structure to have global instability problems. On the one hand, the stiff structure must be designed in such a way that its lateral drift does not exceed that of the soft structure. Because in this case, due to the connection of two structures, more drift is imposed on the soft structure and can cause damage to it. As well as the amount of displacement created in the structure can be a decisive criterion in how to connect two structures. This means that if the amount of this deformation is more than a special amount (which, of course, depends on the equipment available and the seismic force-resisting system) two structures can be connected by viscous damper. In this case, due to the use of high damping values (passive or controlled), in addition to having a lighter stiff structure, the performance of the soft structure can be better controlled.

To find the answer to this question, many studies have been done on the standards and guidelines, and finally the values in Table (1) are suggested.

It should be noted that the recommendations of FEMA 273 [7] and FEMA 356 [8] have been used in the preparation of Table (1). On the other hand, for the consideration of structures with different significance coefficients (according to the Codes [1, 9]), the important factors are proposed as follows Table (2), which must be multiplied by the proposed values. However, due to the special sensitivity of mass and stiff substructures due to the stability problems and uncertainty compared to conventional structures, the proposed values are considered lower than the FEMA recommendation.

3. Procedures for Calculation of Stability Factor

The excessive deformation of the mass structure may have undesirable effects on the stability of the structure. Thus, first, a proper solution should be taken to calculate the structural stability. In this regard, there is a linear buckling analysis in which the structural instability effects of the P-Δ under a particular loading are examined. The buckling analysis is based on the solution of the following Eigenanalysis:

$$\left[K-\lambda K_g\right]\psi=0\Rightarrow\left|K-\lambda K_g\right|=0 \qquad (1)$$

where K is the structure stiffness matrix, K_g is the geometric stiffness matrix, λ is Eigenvalue and Ψ is an Eigenvector, such as buckling mode shape.

Each pair of eigenvalue - eigenvector is called a buckling mode of structure. The eigenvalue λ is called the buckling factor. This coefficient can also be considered as a safety factor. Because if the buckling factor is greater than one, the loads applied to the buckling should be increased; and if this coefficient is less than one, the loads should be reduced

to prevent buckling [10].

In Figure (3), the behavior of a structure is seen with and without regard to the secondary moments of the effect caused by P-Δ. As it is seen, taking into account the decreasing effects of the geometric hardness matrix and the secondary moments reduces the initial stiffness of the pushover structure as well as the expected resistance of the structure. In addition, the behavior of the structure after reaching the yield limit with negative and decreasing stiffness goes down. In this section, how to calculate the amount of these impacts and their effects will be examined.

The problem of structural stability is very important in the design of axial load members. For example, the AISC code provides a safety factor for members with a slenderness ratio of zero is equal to 1.67 and for a very large slenderness ratio equal to 1.92 and between these two limits is the change according to the equation of a quarter-period curve of the sinusoid [11]. However, none of the codes explicitly provides documentary evidence of the reliability ratio versus general stability of the structure, and only ASCE 7-05 explains that the safety factor of 2 has been applied to estimate the maximum stability index [12].

According to a study by Bernal [13] focused on two-dimensional frames and aimed at determining the minimum lateral stiffness needed for the frame, he presented the coefficient of stability with the dynamic modeling of the structure and assuming non-linear behavior for the frame.

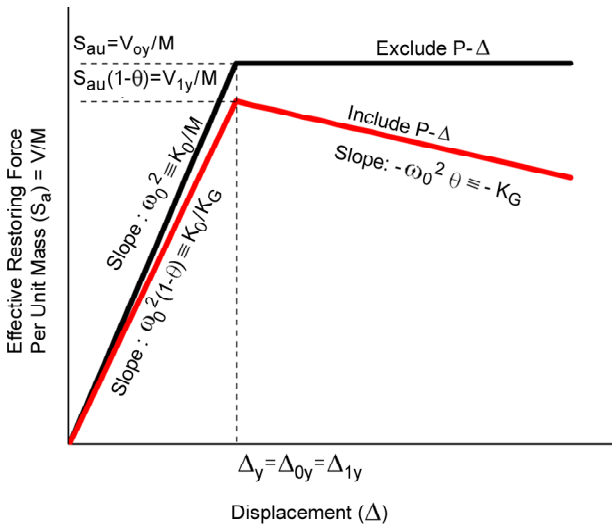

Figure 3. An ideal response of a 1-Story structure, with and without P-Δ effect [12-13].

$$\theta_i = \frac{k_{gi}}{\omega_\circ^2 m_i} \tag{2}$$

where θ_i is the coefficient of stability of the frame after the formation of i^{th} plastic mode. Also, Bernal [14] showed that the stability index can be expressed by its dependence on the mode forms.

$$\theta = \frac{\{\phi_1\}^T [K_g] \{\phi_1\}}{\{\phi_1\}^T [K_\circ] \{\phi_1\}} = \frac{K_{g_1}}{K_1} \tag{3}$$

where $\{\phi_1\}$, the shape of the first mode, K_g, the geometric stiffness matrix, and $K_\circ$, the linear structure stiffness matrix, K_{g_1} and K_1, are the geometric stiffness matrix and the stiffness matrix of the first mode of the structure, respectively.

Accordingly, and in continuation of their work, the empirical equations for calculating the stability index of the linear state $\theta_\circ$ and the stability index corresponding to failure of the frame θ_m are as follows [13-14]:

$$\theta_\circ = \frac{3Ng\tau}{(2N+1)\omega_\circ^2 h}$$

$$\theta_m = \frac{\Omega g \tau}{\omega_\circ^2 h} \tag{4}$$

$$\Omega = \frac{1 + 2N(1 - E/h - 0.5G/h)}{G/h\left[1 + 2N(1 - E/h - 0.67G/h)\right] + \frac{1}{3N}}$$

where N is the number of stories, g is the gravity acceleration, h is the total building height, E/h and G/h shown in Figure (4a), τ is the ratio of total weight to effective seismic weight. Also, based on the relations presented by Bernal [15], Ω indicates the failure mechanism of the structure. However in mass isolation structures, the goal is to preserve the general failure mode and prevent the soft and weak story failure, and therefore in this structure, the theory of weak beam - strong column should be established (Figure 4-b). As a result, in the present study, the values of $\theta_\circ$ and θ_m are equal, and after that, the parametric θ is used.

Also in Equation (4), τ is determined by Equation (5).

$$\tau = \frac{P_u}{W} = \frac{D + 0.5L}{D + 0.2L} \tag{5}$$

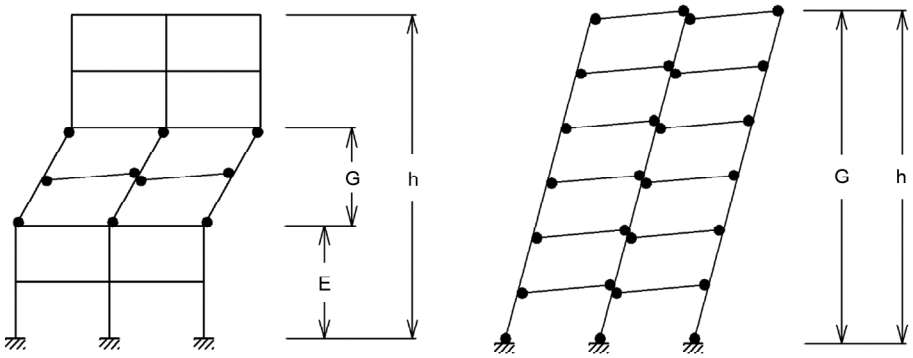

(a) Local Failure [12] (b) Global Failure

Figure 4. Mechanism parameters.

Assuming $L/D=0.4$ (which is reasonable for buildings):

$$\tau = 1.11 \tag{6}$$

Now, by assuming $h=3.3N$ in residential structures, (4a) is simplified as follows:

$$\left.\begin{matrix} h = 3.3N \\ \tau = 1.11 \end{matrix}\right\} \Rightarrow \theta_{\circ} = \frac{1}{\lambda_{\circ}} = \frac{g}{(2N+1)\omega_{\circ}^2} \tag{7}$$

Therefore, using the following equation obtained by the solution of Equation (7), an estimate for the vibration period of the structures can also be obtained.

$$T = 2\pi\sqrt{\frac{(2N+1)}{g\lambda_{\circ}}} \cong 2\sqrt{\frac{(2N+1)}{\lambda_{\circ}}} \tag{8}$$

The critical mechanism for analyzing dynamic stability can be roughly the same as the static failure mechanism due to a pushover analysis with lateral load distributions relative to mass [14]. It has also been shown that the failure mechanism in buildings is statistically independent of the fact that the excitation is near the fault or far from the fault [15].

By comparing this coefficient of stability index based on Equation (3) with the stability factor of the frames mentioned in Equation (1), it can be concluded that:

$$\lambda_1 = \frac{K_1}{K_{g1}} = \frac{1}{\theta} \tag{9}$$

where λ_1 is the coefficient of frame stability in the first mode.

Yield displacement is almost independent of the nonlinear geometric effects of P-Δ [16]. It has also been shown in studies that the initial period (and therefore the initial stiffness) does not play an important role in determining the boundary of instability [14]. As a result, immunity against dynamic instabilities is not guaranteed by controlling the initial elastic stiffness, and a reasonable method of checking safety against this failure mode should be considered by examining the strength and shape of the mechanism of the critical mechanism [14].

Theoretically, a system may persist after a transient response to a dynamic stimulation or even exceed the static stability ($\lambda_s = 1/\theta_{\circ}$), but numerical results show that, for an earthquake excitation, with con-siderable time, the threshold of dynamic instability (λ_d) is much less than λ_s [16]. For example, Castilla and Lopez have suggested that λ_d be considered to be $\lambda_s^{0.5}$ [16-17].

4. Relationships between the Displacement and Overall Stability of Structure Based on Numerical Studies and Pushover Analysis

In this section, by assuming the stability parameter as a design parameter, and not just a check parameter at the end of the design process, in accordance with the desired application of the soft structure, for this structure, the minimum amount of safe buckling factor is determined, and as a result, the force base shear is recommended.

First, the minimum stability factor of the frame must be determined so that, with the assumption of 0.5 to 0.7 percent of the drift for this particular structure, the structural stability is maintained. According to ASCE 7-16, in most structures, if the stability index value exceeds 0.25, the structure has an unstable risk and should be redesigned. This amount of the stability index is equivalent to reducing the stability factor of 4 (see Equation 9), the

structure will be at risk of instability. Accordingly, the stability factor of less than 4 for the structure will be unacceptable, and according to ASCE 7-16, the safety factor for this calculation is equal to 2.

Also, according to the above equations, Equation (10) can be used to estimate the minimum stability factor:

$$\theta_{\max} = \frac{0.5}{\beta C_d - 1} \xrightarrow{\text{usually } \beta=1} \theta_{\max} = \frac{0.5}{C_d - 1} \Rightarrow$$
$$\lambda_{\min} = \frac{C_d - 1}{0.5} = 2\left(C_d - 1\right) \tag{10}$$

For reliability, ASCE allows β = 1 to be conservatively assumed [1]. Regarding Equation (10), having the coefficient *Cd*, the lowest acceptable stability factor can be obtained by assuming a safety coefficient 2 to maintain the stability and expected value for the stability factor.

With the logical assumption and with the use of the Bernal presentation equations, the following method is proposed for soft structure design.

Based on the Bernal studies [13], the nonlinear behavior curve of a structure under the effect of increasing load (pushover curve) can be summarized in the bilinear form below, Figure (5).

In this study, due to the limited variation of the soft substructure displacements in the Mass Isolation Systems (due to their high damping and reliance on the stiff substructure), determination of the stability factor required for these structures in the Collapse Prevention (CP) region has been made. For this purpose, the elastoplastic behavior of the structure that plays the role of the interface between the elastic and plastic behavior in the frame is initially estimated by a third-order curve. This performance boundary in soft structures with limited range variation can be effective in determining the structural stability factor. For this purpose, the performance boundary of the structure between the onset of nonlinear behavior in the frame and the completion of its final capacity is approximated by a third-order equation.

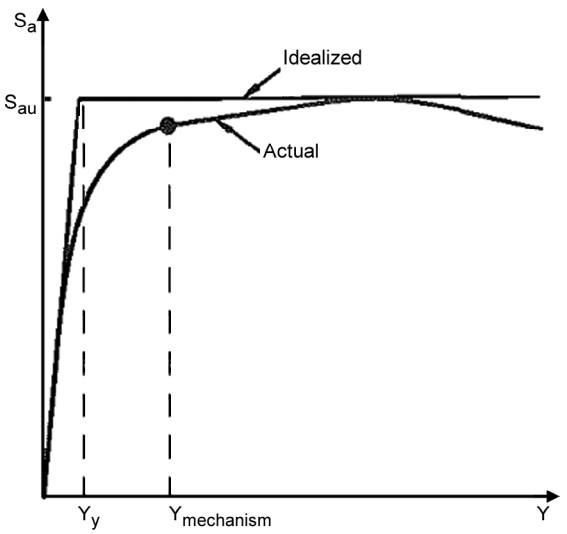

Figure 5. Effective restoring force per unit mass versus generalized displacement [13].

When the effect of P-Δ on the structure is considered, according to Bernal's method, the downward curve of the structural behavior with the assumption that the stability index is equal before and after the start of the mechanism ($\theta_{\circ} = \theta_m = 1/\lambda$).

According to the studies, the maximum permissible lateral displacement limits for structural stability (Δ_c) are estimated on the basis of the lateral bearing capacity at the collapse performance of the structure ($S_c = S_{\max}/I_c$) [12]. $S_{\max}$ in the structural behavior curve, taking into account the effect of P-Δ, the peak point of the behavioral curve of the structure and $I_c = 1.7$, is the ratio of the reduction of the bearing capacity of the lateral structure at its collapse rate for static to dynamic behavior [13]. Using this method, the boundary value of the structural displacement is determined by maintaining the stability under the influence of dynamic loads. The displacement level of collapse prevention performance (Δ_{cp}) can be calculated assuming a resistance loss coefficient (α) relative to the maximum lateral bearing load capacity of the structure ($S_{\max}$) (lateral bearing capacity of the structure in this range is assumed $S_{cp} = 0.8S_{\max}$ [18]). Since the over-strength factor of the structure (Ω) is assumed, the design load of the structures can also be calculated $\left(S_d = S_{\max}/\Omega\right)$.

Assuming a general failure for the soft structure and consequently the uniformity of the stability index before and after entering the plastic behavior, assuming the response modification coefficient (R=4.5) and the design acceleration (A=0.35 g), the curves of Figure (6) are obtained for the four-floor structure with different stability factors.

$$\lambda = 30 \rightarrow T = 2\sqrt{\frac{2N+1}{\lambda}} = 1.1$$
$$\frac{S_u}{g} = \Omega \frac{ABI}{R_u} = 2 \times \frac{0.35 \times 1.9 \times 1.0}{4.5} = 0.3 \tag{11}$$

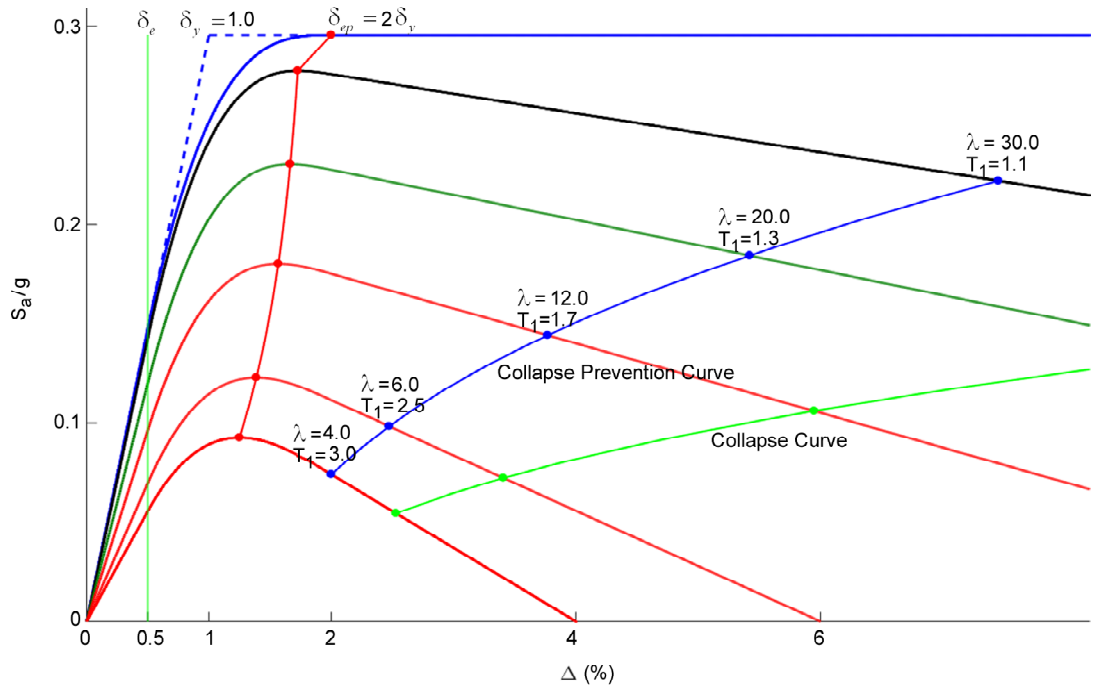

Figure 6. Proposed curves for pushover behavior of structures with a specific stability factor for the four-floor structure.

In Figure (6), the deformation of the yield limit in the bilinear behavior model is assumed in accordance with the recommendations of Dimopoulos et al. [19], ($\Delta_y = 1\%$).

The collapse curve represents the limit value of the available displacement for the structure. It is assumed that, if the strength of the structure decreases so much that the ratio of the maximum structural strength to the existing strength is equal to the ratio of $I_c = 1.7$, the structure will reach its final acceptable performance. It is also assumed for the collapse prevention curve that if the structure's resistance to 80% of the maximum resistance of the structure decreases, the structure has reached its collapse prevention rate. These curves are normalized to the displacement of the elastic limit, Δ_e ($\Delta_e = \Delta_y / \Omega$), and also the upper curve representing the structure, regardless of the behavior of P-Δ. To calculate the period, the proposed formula is used, and the vertical axis in this figure represents the effective restoring force per unit mass, $S_a = V/M$, and the endpoint of the linear behavior is also considered as the acceleration of the design of the structure, $S_d = ABI/R$ [9], which $A = 0.35$ g is considered as the design basis acceleration, and indicates the earthquake response factor based on Iranian Code Standard No. 2800 [9]and based on the calculated period with the proposed relationship, $I = 1.0$ is the importance factor and $R = 4.5$ is the response modification factor [1]. Conventionally designed structures usually have a stability factor $12 \le \lambda \le 20$, and for the soft structure, the goal is to bring the structure to $\lambda = 4$.

Therefore, in order to design a soft structure in a recent method, according to the proposed equation for pushover behavior and assuming global failure behavior, the amount and location of the maximum acceleration (S_{au}) are calculated according to the stability factor λ. Then the acceleration value at the collapse limitation, which is considered as the collapse acceleration (S_{ac}) (assuming the $I_c = S_{au}/S_{ac} = 1.7$ ratio, according to the Bernal recommendation), is calculated in λ; the acceleration value is also calculated at the collapse prevention acceleration (S_{acp}), assuming the ratio of $S_{acp}/S_{au} = 0.8$ to be calculated.

Therefore, for the nonlinear behavior of the hypothesis of the 4-class structure, with the assumption $\Omega = 2$, the following relations are presented. These relationships are based on numerical analysis and linear interpolation

$$T = 2\sqrt{\frac{(2N+1)}{\lambda}} < \sqrt{2N+1} \tag{12}$$

$$\Delta_c = (0.8\lambda + 2.0)\Delta_e, \text{ or: } \lambda = 1.2\left(\frac{\Delta_c}{\Delta_e}\right) - 2.5 > 4 \tag{13}$$

$$\Delta_{cp} = (0.4\lambda + 2.5)\Delta_c, \text{ or: } \lambda = 2.5\left(\frac{\Delta_{cp}}{\Delta_c}\right) - 6.25 > 4 \quad (14)$$

5. The Soft Structure Design Method

Because an additional damper to a stiff structure connects this structure, it is one of the high-damping structures. Therefore, according to Chapter 18 of the ASCE 7-16 code [1], assuming the use of a damper in all stories (preferably in the case of a mass isolation system this will not be the case, and depending on the height of the structure, at least three elevations of the damper are used) and using the ELF method:

Assuming the design of a 4-story structure with $\lambda = 6$, $\Delta_y = 1.0\%$ and using Equation (15), this structure should be able to withstand the $\Delta_{cp} = 2.45\%$ drift under critical conditions. It should be noted that in the design of a soft structure in practice, this structure is designed for the drift of about 1%, which should be provided by a damper and connecting to the stiff structure. However, in critical conditions and into the nonlinear behavior of the two structures, the soft structure should withstand, without any damage. Therefore, assuming that this structure should eventually be able to withstand 2.45% drift, the ELF method used [1]:

$$\begin{aligned}
&H = 13.2\,m,\\
&T_1 = 2\pi\sqrt{\frac{2N+1}{\lambda g}} = 2\pi\sqrt{\frac{2\times 4+1}{6\times 9.806}} = 2.46\\
&R = 4.5, I = 1.0, \Omega_\circ = 3 \rightarrow \mu_{\max} = 1.5 \Rightarrow \mu_D = 1.5\\
&T_{1D} = T_1\sqrt{\mu_D} = 3.01\\
&T_s = 0.7 \rightarrow q_H = 0.67\frac{T_s}{T_1} = 0.19\\
&\beta_I = 3.5\% \rightarrow \beta_{HD} = 3.85\%\\
&\beta_{V1D} = 42\% \rightarrow \delta_{1D} = 2.07\%, C_{S1} = 0.0335
\end{aligned} \quad (15)$$

The above parameters can be defined according to ASCE7-16 as follows [1]: $\mu_{\max}$ is the maximum effective ductility demand according to section 18.7.3.4, μ_D is the effective ductility demand that according to section 18.7.3.3 shall not exceed the maximum effective ductility demand ($\mu_{\max}$). T_{1D} is the effective fundamental mode period at the design earthquake (section 18.7.2.2). q_H is the hysteresis loop adjustment factor, as defined in section 18.7.3.2.2.1. β_I is component of effective damping of the structure caused by the inherent dissipation of energy by elements of the structure, at or just below the effective yield displacement of the seismic force-resisting system; β_{HD} is component of effective damping of the structure in the direction of interest caused by post yield hysteresis behavior of the seismic force-resisting system and elements of the damping system at effective ductility demand, μ_D; and β_{V1} is component of effective damping of the first mode of vibration of the structure in the direction of interest caused by viscous dissipation of energy by the damping system, at or just below the effective yield displacement of the seismic force-resisting system (section 18.7.3.2). δ_{1D} is the design story drift caused by the fundamental mode of vibration of the structure in the direction of interest (section 18.7.2.3.2) and finally C_{S1} is the fundamental mode ($m = 1$) seismic response coefficient (section 18.7.1.2.4).

As can be seen, to achieve the target lateral drift of approximately 2%, it should provide 42% of the additive damping, whereas, according to the recommendation of this code [1], attenuation damping should not be more than 35% in total, while with this additive damping, the total attenuation is about 60% damping (Eq. 18.7-45 [1]). In fact, in order to achieve this goal, it has to add more damping to the structure. However, according to the above calculation, the structure should eventually be set to 1% drift, while according to the ELF method, even with the assumption of providing 70% of the additive damping. This suggests that for the correct analysis of these systems, firstly, the nonlinear dynamics analysis and non-classical damping methods must be used; secondly, in order to achieve this goal, Rayleigh's damping ratio should be more than 100% for this structure (Eq. 18.7-45 [1]). Ziyaeifar et al. [6] have shown that this ratio of damping is greater than the stall damping, and it is proved by non-classic alanalysis that although this damping rate is very high, it will not cause high relative damping and the structure will completely change the frequency and behavior.

Therefore, to design the soft structure, the following step-by-step approach is recommended:

1. The maximum permissible lateral displacement for structural stability (Δ_c) or the lateral displacement to collapse prevention (Δ_{cp}) is chosen as the design target (it should be noted that Δ_c is the

maximum allowable lateral displacement for structural stability, but soft substructure is designed for Δ_{cp} and this threshold for soft substructure displacement should be controlled by stiff substructure and damper control).

Note: It should be noted that the choice of Δ_c or Δ_{cp} depends on the available facilities to control the displacement of the soft substructure. In addition, the stability factor obtained for the modeled structure should be considered and the instability threshold value should be avoided.

2. The yield lateral displacement in the bilinear curve (Δ_y), is assumed.
3. Then the stability factor of the structure (λ) (assuming elastic displacement $\Delta_e = \Delta_y / \Omega$) is calculated by Equations (13) or (14). Of course, the stability factor can be assumed, and then Δ_c and Δ_{cp} can be obtained from these equations.
4. Calculate the approximate period of the structure using Equation (12).
5. The seismic base shear according to standard criteria is obtained using the period calculated in step 4 [1, 9].
6. The target displacement is controlled using dynamic analysis methods and after the soft substructure is connected to the designed stiff substructure with the desired placement of dampers, Figure (7).

For example, consider a 5-story structure shown in Figure (8).

To calculate the seismic load of a soft structure, the following procedure is applied [9]:

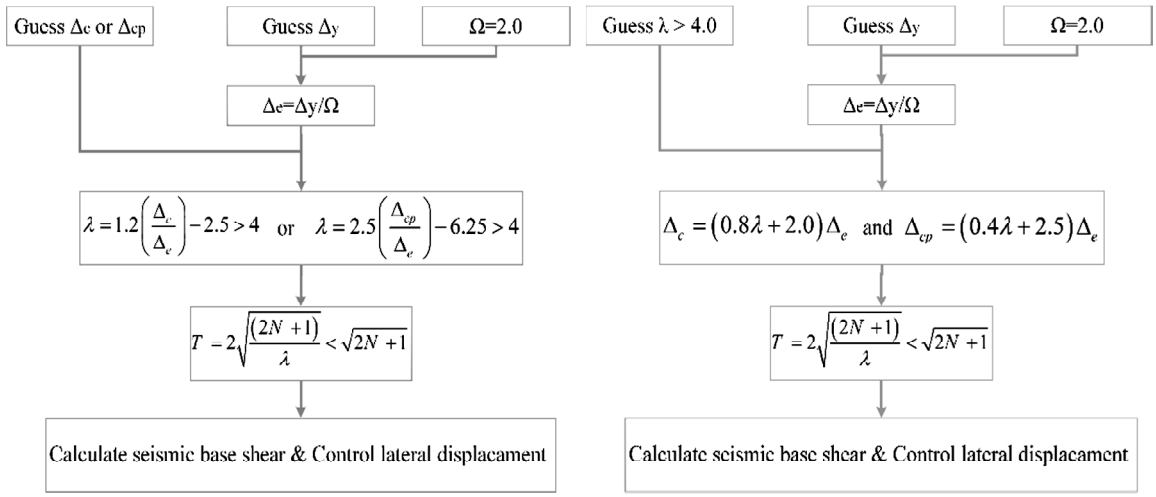

(a) The Choice of Δ_c or Δ_{cp} (b) The Choice of λ

Figure 7. The suggested design procedure.

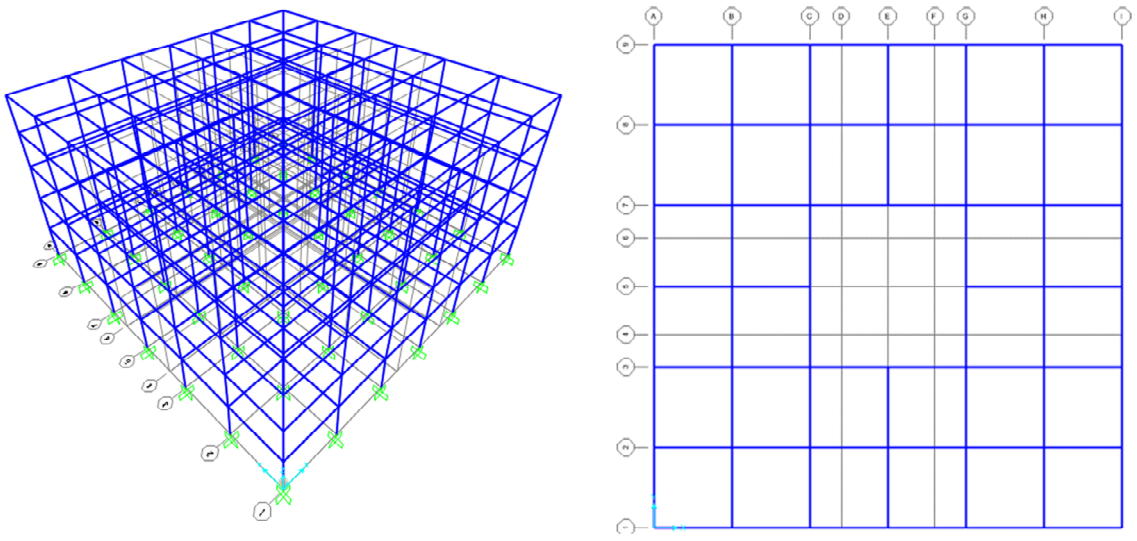

(a) 3D View of the Soft Structure (b) The Plan of the Soft Structure

Figure 8. A view of the 5-story structure of the investigated.

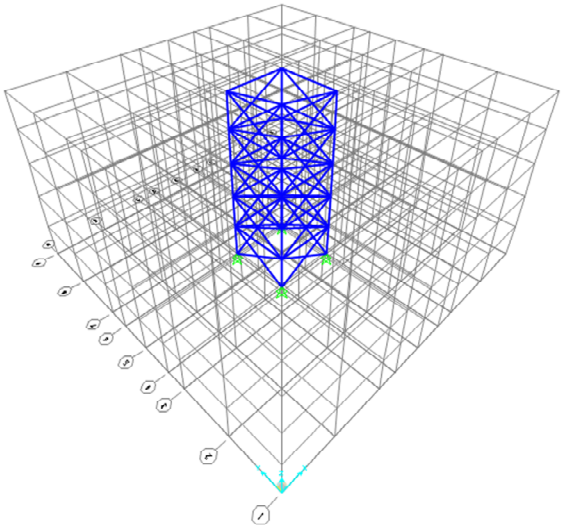

(c) 3D View of the Stiff Structure

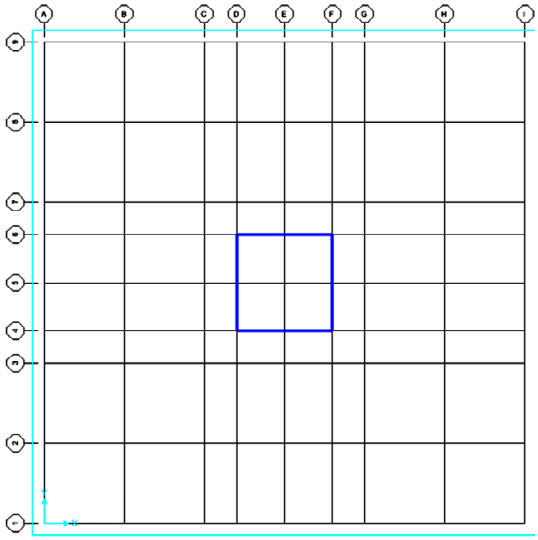

(d) The Plan of the Stiff Structure

Figure 8. Continue

$$Mass\ SubSystem:$$

$$guess:\begin{cases}\lambda=6\\ \Delta_e=0.5\%\end{cases}\Rightarrow\begin{cases}T=2\sqrt{\dfrac{2N+1}{\lambda}}=2.7\\ \Delta_c=(0.4\lambda+2.0)\Delta_e=2.2\%\\ \Delta_{cp}=(0.2\lambda+2.5)\Delta_e=1.85\%\end{cases}$$

$$Guess:(Soil\ Type:III\ \&\ A=0.35g\ \&\ I=1.0\ \&\ R=4.5)\rightarrow$$

$$T_\circ=0.15,\ T_s=0.7,\ S=1.75,\ S_\circ=1.1$$

$$\left.\begin{array}{l}T=2.7>T_s\rightarrow B_1=(S+1)\dfrac{T_s}{T}=0.71\\ T_s<T\le 4s\rightarrow N=\dfrac{0.7}{4-T_s}(T-T_s)+1=1.4\end{array}\right\}\rightarrow B=B_1N=1.02 \tag{16}$$

$$C=\frac{ABI}{R}=0.079$$

Due to the fact that the stiff structure must be connected to the soft structure by the damper and in order to achieve a period difference between the two structures, it is assumed that the stiff structure is designed with 30% of its seismic weight.

Assuming the seismic loads above, two structures are designed and the results are summarized as follows, Table (3).

In the first step, by pushing the soft structure, we compare the resulting curve with the proposed curve, which yields the following results, Figure (9).

As can be seen, the proposed curve has a good fit with the curve of the structure and in drawing this curve with respect to the actual curve of the structure, $\Delta_e=1.23\%$ and $V_{max}=3293.53\,kN$.

In the next step, in order to obtain an initial estimate of the optimal damping for connecting the two structures of the relationships provided by Ziyaeifar et al. [6] will be used. To do this, at first, the two structures are rigidly joined to each other, and the period and the weight of the structure are calculated, which yields the following results:

$$T_p=1.317s\rightarrow\omega_p=4.77\,rad/s$$

$$\Gamma_1=0.75,\quad W_p=27248.5\,kN\Rightarrow$$

$$M_p=\frac{\Gamma_1 W_p}{g}=2094.93\,ton$$

$$\left.\begin{array}{l}C_{Stall}\approx 2\overline{\xi}_P^{Stall}M_P\omega_P\\ \overline{\xi}_P^{Stall}=0.25\end{array}\right\}\Rightarrow C_{Stall}=2\times 0.25\times 2094.93\times 4.77\times\left(4\frac{\sqrt{2}}{2}\right)\cong 1750\ N.s/mm \tag{17}$$

Mass and stiff substructures are connected to each other by eight dampers (two on each side) on the 4th floor. The reason for using the arrangement of eight dampers is to prevent locking in dampers and distributing force in the diaphragm.

The soft structure with different damping ratios is connected to the stiff structure and the nonlinear time history analysis is analyzed for the seven accelerations mentioned in Table (4). Initially, the accelerometers in the period of 0.2 to 1.5 times the period of the two structures are matched to the spectrum of Iranian Code Standard No. 2800 [9] and scaled to design basis acceleration 0.35 g, Figure (10).

Finally, the average results of seven accelerations can be evaluated as follows, Figures (11) and (12).

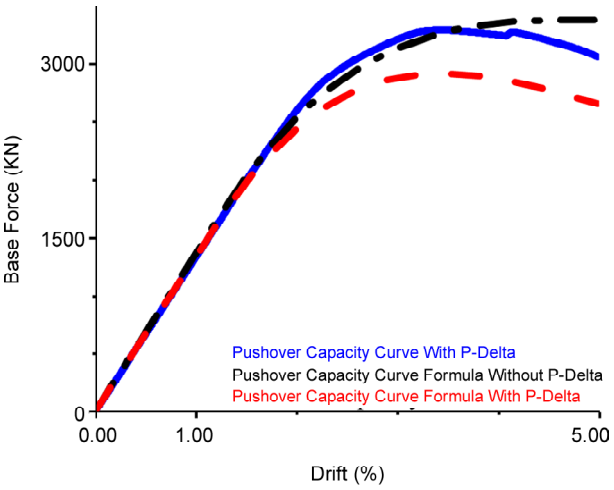

Figure 9. Comparison of the structure pushover curvature with the proposed formulation.

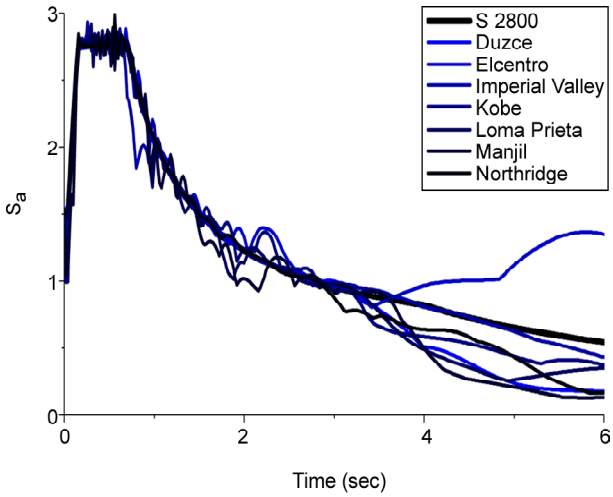

Figure 10. Design spectral of matched time histories ($0.05 \leq T \leq 3.75$).

Table 3. Sample structure calculations.

Structure	Mass SubSystem	Stiff SubSystem			
Element	Column	Beam	Column	Beam	Brace
Story 1	Box260X10	IPE180	Box180X8	IPE270	Box140X8
Story 2	Box240X10				
Story 3	Box220X10				
Story 4	Box200X10				
Story 5	Box180X10				
Partial Fixity	50%		0%		
T (sec)	2.51		0.342		
λ	6.31		20.65		
T Eq.	$2\pi\sqrt{\frac{2N+1}{g\lambda}}=2.65$		---		
Δ_c Eq.	$\Delta_c=(0.4\lambda+2.0)\Delta_e=4.5\%,(\Delta_e=1.0\%)$		---		
Δ_{cp} Eq.	$\Delta_{cp}=(0.2\lambda+2.5)\Delta_c=3.8\%,(\Delta_c=1.0\%)$		---		

Table 4. Characteristics of used time histories [20-23].

Earthquake Name	Station Name	Year	M	PGA (g)
Duzce	Bolu	1999	7.1	0.82
El Centro	Elcentro Array #9	1940	6.9	0.31
Imperial Valley	Elcentro Array #11	1979	6.5	0.38
Kobe	Nishi Akashi	1995	6.9	0.51
Loma Prieta	Capitola	1989	6.9	0.53
Manjil	Abhar	1990	7.4	0.51
Northridge	Beverly Hills	1994	6.7	0.52

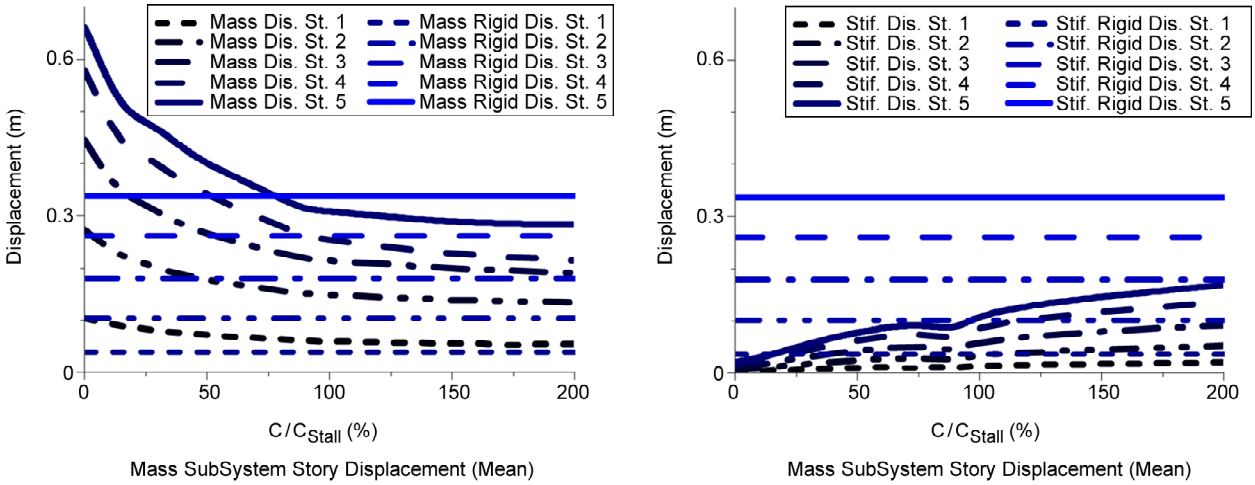

Figure 11. The change in the mean of the maximum story displacement for seven time histories in terms of the damping coefficient of the dampers.

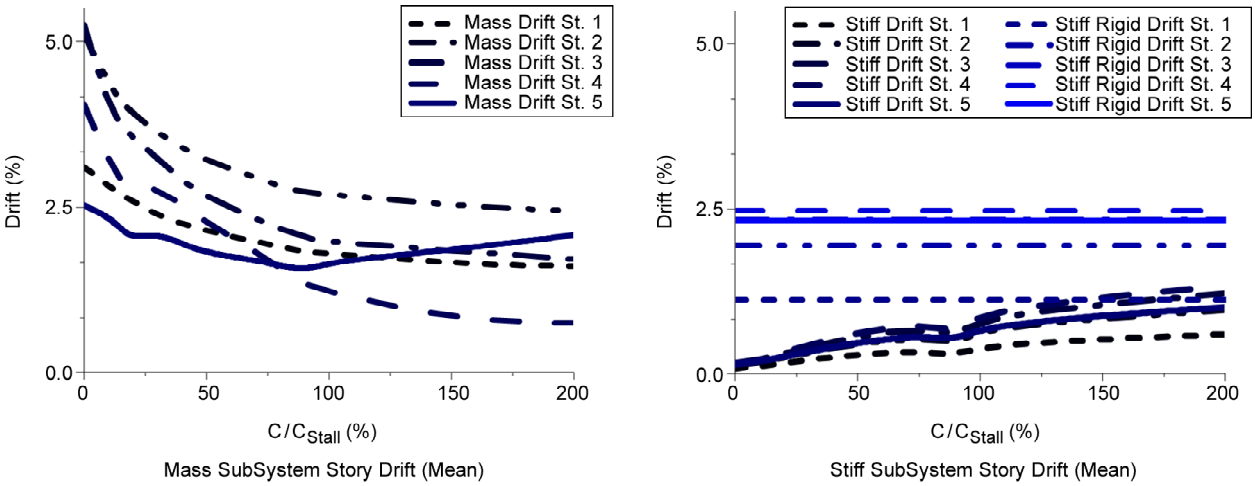

Figure 12. The change in the mean of the maximum story drift for seven time histories in terms of the damping coefficient of the dampers.

It should be noted that in the above figures, Mass Rigid means that the two substructures are rigidly connected to each other on all floors.

As shown in the figure above, an increase in the damping coefficient rapidly reduces the displacement of the soft structure, while the displacement of the stiff structure has not increased significantly. However, after reaching the optimum damping point, the intensity of the change of displacement in the soft structure is reduced, while at the same time the intensity of the change of displacement of the stiff structure increases, but in any case, the amount of this displacement differs significantly from the rigid connection of the two structures. However, here the criterion is to determine the appropriate performance level for a soft structure, which, according to Table (3), is the optimum reach for the threshold of 3.8% or 0.63 m roof displacement. Thus, the optimum relative damping coefficient of 0.9 is optimally selected as the optimum performance point. However, it should be noted that to achieve this level of displacement in the soft structure, we needed to provide more damping than the optimal damping, there was no preventive performance. Because, as discussed earlier, the stiff structure did not suffer from unacceptable deformation and another important point is that, with this level of damping, the structure mode, as shown in Figure (13), has not changed significantly and the dampers used have not locked the 4th story displacement. Another important point in this figure is that the relative damping coefficient of about 0.8 is the optimum damping. The roof displacement in this case, as well as the 4th story (the connection of the dampers), are

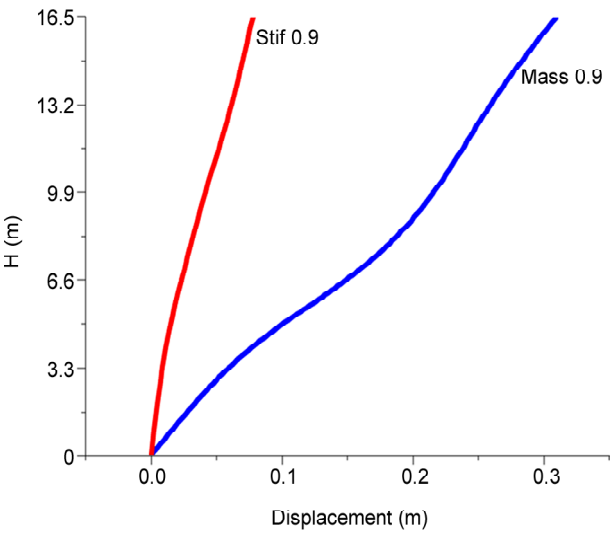

Figure 13. The average displacement curve of the stories in the relative damping coefficient of 0.9 versus optimal damping.

less than the displacement in the rigid connection, and this point can be a significant functional point for determining the amount of damping that will be carefully considered in the next papers.

In addition, according to Figure (14), the acceleration of the stories of both structures relative to their rigid connection is always smaller or sometimes at a very small difference, which indicates that the flexural connection of these two structures relative to their rigid connection also controls acceleration, especially in upper floors. Another noteworthy point is that in the near of optimum damping, the lowest acceleration of stories in all stories is observed, and after this damping ratio, the acceleration increases (due to limited variations in the displacement of the soft structure stories, Figure (11), and the points previously mentioned). However, this increase is not significant and reaches a saturation level.

In Figure (15), the curve shows the maximum variation in the relative displacement of the two head dampers and the force created therein. At least the relative displacement is desirable for optimum performance of the dampers of about 15 cm. As can be seen, we have achieved this level of displacement near optimum damping, while the maximum force created in the dampers is about 80 tons.

These results show that by using the high damping ratio, the drift of the structure can be reduced to the optimum level by non-classical and nonlinear dynamics analysis, and the performance of both structures is also better than their rigid connection, while the soft structure is as smooth as possible.

Finally, it should be noted that the proposed method is an initial design process that is being studied in more detail, but according to studies so far, this method is limited to short to mid-high structures (approximately up to 20-story). Also, considering that the minimum possible stability factor has been used to design the mass substructure, this structure should have absolutely no irregularities.

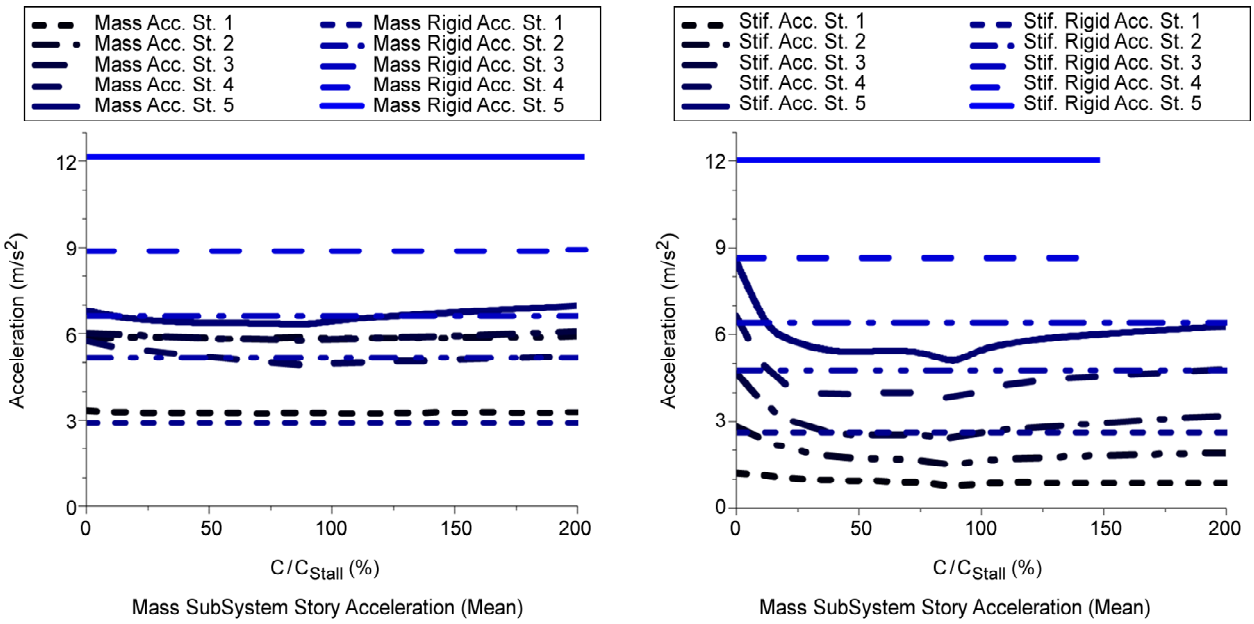

Figure 14. The mean change in the maximum story acceleration for seven time histories in terms of the damping coefficient of the dampers.

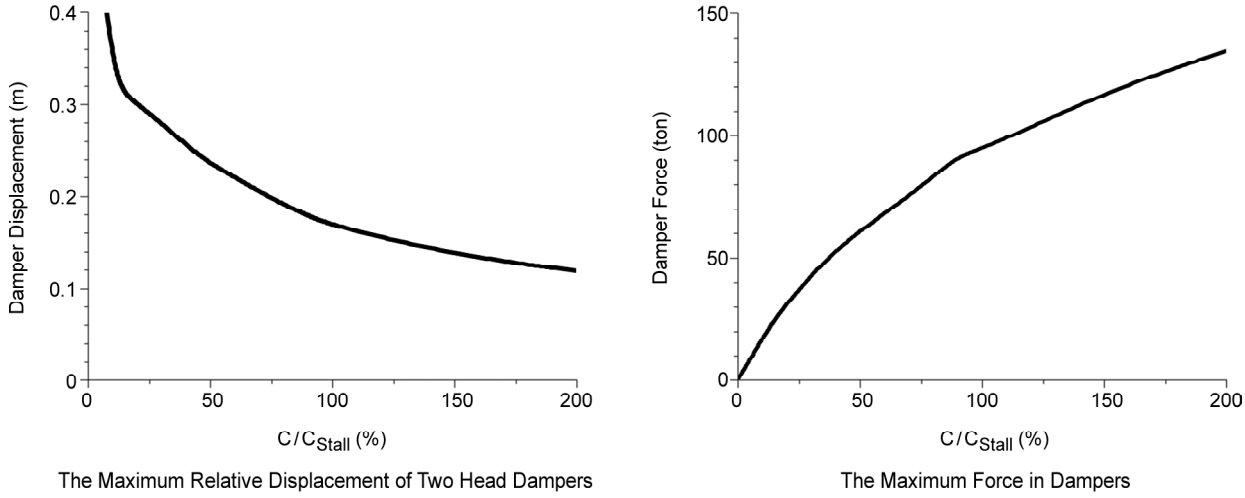

Figure 15. The curve of maximum variation of force and displacement of two head dampers.

6. Conclusion

In this paper, Mass Isolation System (MIS) is considered, which consists of two substructures that must be periodically disaggregated to achieve optimal performance, so that the dampers between the two substructures can have good efficiency.

In order to make the periodic difference between the two substructures and to reduce the earthquake force level, the soft subsystem was designed to increase the period and flexibility of the structure by maintaining its stability. In this regard, a relation was proposed for calculating the period of moment frames in terms of structural stability factor.

Subsequently, the posh-over behavior of the structure was estimated mathematically and based on this behavior, a relation was presented to calculate the structural drift at the threshold of collapse and collapse prevention.

Finally, a method for designing a soft infra-structure in an MIS is presented and evaluated on a 5-story Mass Isolation Structure, and the results show the feasibility of this design method.

Based on the modeling, the following results can be expressed:

Increasing the damping coefficient in dampers should significantly reduce the story displacement of the mass substructure, while there is no significant increase in the displacement of the stiff substructure, and after reaching the stall damping ratio introduced in the author's previous articles, the displacement of the soft structure will not change significantly. Also, the story acceleration of both substructures will be less than the case where the two substructures are converted into a single structure by the story rigid connections. In addition, this method can achieve a relative displacement of 15-20 cm at the two ends of the damper, while the required force in dampers will be within acceptable limits in this type of dampers.

Finally, it should be noted that this method can only be used in short to mid-high structures. Besides, in the process of achieving the presented relation-ships, hypotheses have been made that need to be evaluated and reviewed more accurately by performing dynamic analysis and IDA.

References

1. ASCE (2017a) *Minimum Design Loads and Associated Criteria for Buildings and Other Structures: ASCE/SEI 7-16*. In: Reston, Virginia: Published by American Society of Civil Engineers.

2. EuroCode (2004) Design of structures for earth-quake resistance - Part 1: General rules, seismic actions and rules for buildings. *EuroCode 8*, **3**, 229p., BSI Standards Publication.

3. Christenson, R.E., Spencer, Jr., B.F., Hori, N., and Seto, K. (2003) Coupled building control using acceleration feedback. *Computer-Aided Civil and Infrastructure Engineering*, **18**(1), 4-18, doi:http://dx.doi.org/10.1111/1467-8667.00295.

4. Yuji, K., Keizo, N., Masanori, I., Tamotsu, M., and Hirofumi, S. (2004) Development of connecting type actively controlled vibration control devices and application to high-rise triple buildings.

Engineering Review, **37**(1).

5. Ziyaeifar, M. (2002) Mass Isolation, concept and techniques. *European Earthquake Engineering*, **2**(1), 43-55.

6. Ziyaeifar, M., Gidfar, S., and Nekooei, M. (2012) A model for mass isolation study in seismic design of structures. *Structural Control and Health Monitoring*, **19**(6), 627-645, doi:http://dx.doi.org/10.1002/stc.459.

7. ATC-33 (1997) NEHRP Guidelines for the Seismic Rehabilitation of Buildings (FEMA 273). Applied Technology Council (ATC-33 Project), Washington, D.C., Federal Emergency Management Agency.

8. FEMA (2000) Prestandard and Commentary for the Seismic Rehabilitation of Buildings (FEMA 356), In Washington, D.C., Federal Emergency Management Agency.

9. BHRC (2014) *Iranian Code of Practice for Seismic Resistant Design of Buildings, Standard No. 2800*. 4th Ed., Tehran: Road, Housing and Urban Development Research Center.

10. CSI (July 2015) *CSI Analysis Reference Manual*.

11. AISC-ANSI, A. (2010) *Specification for Structural Steel Buildings (ANSI/AISC 360-10)*. Chicago (IL), American Institute of Steel Construction.

12. ASCE (2010) Commentary for Chapters 11-22 (Seismic). *Minimum Design Loads for Buildings and Other Structures*.

13. Bernal, D. (1992) Instability of buildings subjected to earthquakes. *Journal of Structural Engineering*, **118**(8), 2239-2260, doi:http://dx.doi.org/10.1061/(ASCE)0733-9445(1992)118:8(2239).

14. Bernal, D. (1998) Instability of Buildings during seismic response. *Engineering Structures*, **20**(4-6), 496-502, doi:http://dx.doi.org/10.1016/S0141-0296(97)00037-0.

15. Bernal, D., Nasseri, A., and Bulut, Y. (2006) Instability inducing potential of near fault ground motions. *SMIP06 Seminar Proceedings*.

16. Bernal, D. (1987) Amplification factors for inelastic dynamic P-Δ effects in earthquake analysis. *Earthquake Engineering and Structural Dynamics*, **15**, 635-651.

17. Castilla, E. and Lopez, O. (1980) Influence of gravity loads in seismic response (in Spanish). *Bol. IMME*, **18**(67), 3-18.

18. ASCE (2017b) S*eismic Evaluation and Retrofit of Existing Buildings (ASCE/SEI 41-17) 518*. doi:10.1061/9780784414859.

19. Dimopoulos, A.I., Bazeos, N., and Beskos, D.E. (2012) Seismic yield displacements of plane moment resisting and x-braced steel frames. *Soil Dynamics and Earthquake Engineering*, **41**, 128-140, doi:http://dx.doi.org/10.1016/j.soildyn.2012.05.002.

20. ATC (2008) *Quantification of Building Seismic Performance Factors - ATC-63 Project Report 90% Drift (FEMA P695)*. (A.T. Council Ed.): Federal Emergency Management Agency.

21. Chopra, A.K. (2007) *Dynamics of Structures Theory and Applications to Earthquake Engineering*. (3rd Ed.): Pearson Education.

22. COSMOS (2018) *Strong Motion Virtual Data Center*. Retrieved from www.strongmotioncenter.org/vdc/scripts/stnpage.plx?stations=28.

23. PEER (2018) *NGA-West2 PEER Ground Motion DataBase*. Retrieved from htpps://ngawest2.berkeley.edu.